COBEM 2023 27TH INTERNATIONAL CONGRESS OF MECHANICAL ENGENEERING

ABCM Brazilian Society of Mechanical Sciences and Engineering
27th ABCM International Congress of Mechanical Engineering
December 04-08, 2023, Florianópolis-SC, Brazil

COB-2023-0400
NUMERICAL STUDY OF A REGENERATIVE COOLING JACKET IN A SCRAMJET INLET

Marco Antônio Esteves dos Santos
Guilherme Ribeiro Borges
Aeronautics Institute of Technology. Praça Marechal Eduardo Gomes, 50 Vila das Acácias, 12228-900. São José dos Campos/SP – Brasil.
emails: marco.santos@ga.ita.br, gbribeiro@ita.br

***Abstract**: The study addresses the challenge of overheating in Scramjet engines through regenerative cooling. The central focus lies in the application of a channel configuration to mitigate high temperatures at the attack edges and engine ramps, employing hydrogen as refrigerant. Scramjet engines operate at hypersonic speeds, being powered by atmospheric oxygen. However, such extreme conditions generate excessive temperatures in the inner parts of the engine, resulting in wear and deterioration that affect performance and service life. To overcome this problem, the study proposes regenerative cooling, a technique that involves the circulation of a refrigerant through internal motor channels to dissipate excessive heat. The study explores the implementation of a specific channel geometry as a strategy to reduce critical temperatures. The results demonstrate that the geometry of the rectangular channel with dimensions of 2x2 mm is the most appropriate, establishing a precise relationship between flow, entropy and the motor profile.*

Keywords: Channel Geometry, Hydrogen, Scramjet Engine, Regenerative cooling, Hypersonic Propulsion.

1 INTRODUCTION

The search for development in the aerospace sector has been driven considerably by increased interest in hypersonic propulsion systems. According to (Bonelli et al., 2011), hypersonic propulsion technology has been pointed out as the most promising both to reduce travel time in long-distance civilian flights, and as a Single Stage to Orbit (SSTO) vehicle. There are numerous possibilities for the application of hypersonic propulsion, and a variety of approaches are being explored, among them stands out the technology of Scramjets engines. These engines demonstrate superior efficiency at high speeds compared to conventional rocket engines, operating in a manner analogous to Ramjet engines, but at extremely high speeds. The development of Scramjets engines has attracted increasing interest in the aerospace community due to its revolutionary potential in hypersonic propulsion (Ferri, 1968). These engines can operate at speeds above five times the speed of sound, offering significant promise in the field of aviation and space exploration (Nasa, 2006). However, one of the fundamental challenges faced by these engines is the efficient management of heat generated during the combustion process at high speeds. In the context of Scramjets engines, regenerative cooling plays a vital role in mitigating the intense heat generated during hypersonic combustion. Unlike conventional jet engines, which use a combination of ambient air and fuel to cool their components, Scramjet engines employ a more sophisticated and efficient method.

The implementation of regenerative cooling in Scramjet engines presents a number of design challenges and considerations. The first crucial aspect is the development of advanced, heat-resistant materials capable of withstanding the extreme temperature and pressure conditions found at high speeds. In addition, it is necessary to carefully design the geometry of the cooling channels to optimize heat transfer and minimize resistance to air flow. However, it is important to note that hypersonic propulsion also presents many engineering and technological challenges, such as thermal management, extreme aerodynamic resistance and materials capable of withstanding the extreme temperature and pressure conditions encountered at high speeds. Recently, research in the field of Scramjet engines has focused on advanced cooling and heat transfer strategies to improve fuel efficiency and overall performance. In this context, several studies have explored different approaches to optimize cooling cycles and understand heat transfer mechanisms in Scramjet engines.

A study conducted by (Bao et al., 2010) investigated a re-cooled cooling cycle for Scramjet engines to reduce fuel consumption during the cooling process. They proposed an analytical model to evaluate the flow in rectangular ducts, focusing on the influence of geometry on cycle performance. Comparing the Re-Cooled cycle with traditional regenerative cooling, the researchers concluded that duct size plays a crucial role, with smaller diameters showing higher efficiency. However, they stressed that the Re-Cooled cycle demands more pumping energy. In addition, the study emphasized the importance of considering thermal and Mach number constraints in the design of the Re-Cooled cycle, highlighting the complexity of the interactions between the parameters.

(Han et al., 2022) proposed a comprehensive program for thermal analysis of Scramjet aircraft with regenerative cooling channels. The program incorporates several factors, including thermal aerodynamics, cooling channels, combustion heating and heat transfer to the aircraft's internal components. The study developed numerical methods for thermal analysis of flow and structures, applying the heat generated by combustion on internal surfaces. The program made it possible to evaluate the temperatures of each component during specific flight conditions, highlighting the importance of combined thermal analysis for the proper development of Scramjet engines.

Exploring heat transfer under supercritical conditions, (Sun et al., 2019) focused on the analysis of heat transfer of hydrocarbon fuels in a horizontal square cooling channel. Using a computational fluid dynamics (CFD) model, they investigated the flow dynamics and heat transfer of RP-3 aviation kerosene under asymmetric heating and buoyancy effects. The study demonstrated that the variation of the density of the fuel with the temperature induces significant effects of buoyancy in the heat transfer, highlighting the influence of secondary flows in the optimization of the heat transfer.

(He et al., 2023) addressed the importance of studying the heat transfer mechanisms coupled in the regenerative cooling system of Scramjet engines. The article emphasized the coupling relationship between combustion and heat transfer as a critical factor to optimize cooling and combustion performance. Pyrolysis and fuel flow rate were discussed as significant influences on heat transfer in the cooling channel. The study recommended strategies, such as adjusting the cooling channel layout and suppressing coking, to achieve optimal performance. The conjugate thermal analysis was pointed out as a valuable tool to evaluate thermal protection systems.

In the incessant search for improving efficiency and performance, as demonstrated, the method covered in this article is located at the intersection between CFD and Python programming, being applied to a 2D model. The main objective of this approach is to determine the minimum entropy and flow in the system. Data such as altitude, fluid and Mach number are already predefined. With this, variations in flow and entropy will be presented in different specific configurations of the channel geometry.

2 METHODOLOGY

The methodology in question shows remarkable prominence in the presentation of the formulations that govern the system, addressing both the fundamental characteristics of the hydrogen element and its application in the context of the CFD model. In this context, we highlight the use of a criterion parameter, essential to ensure the convergence of the problem addressed. In addition, the methodology covers the exposition of the equations related to the flow in a channel of one-dimensional nature and provides a detailed representation regarding the determination of the geometric dimensions of this channel.

2.1 Characteristics of hydrogen as a coolant at high temperatures and its thermodynamic properties.

Hydrogen has been a clear choice for many researchers regarding Scramjet engines, due to its versatility and performance in high temperature applications (Walker, 2004). Its unique features make it an attractive choice for cooling systems in extreme temperatures. In this context, Figures 1, 2, 3 and 4 highlight the thermodynamic properties of hydrogen as a function of temperature and constant pressure, according to (Labib and King, 2015).

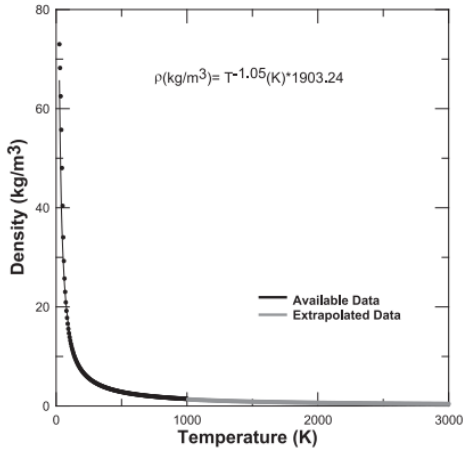

Figure 1. Density.

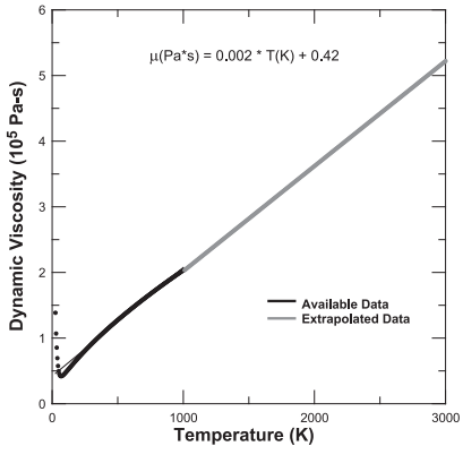

Figure 2. Dynamic viscosity.

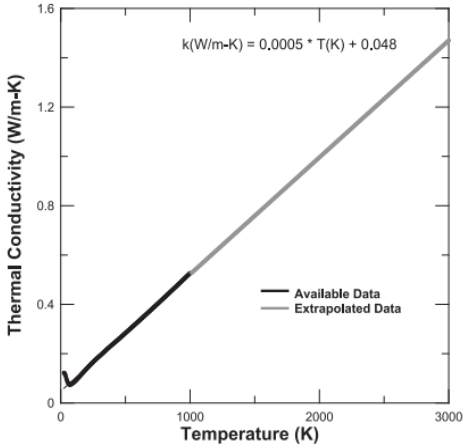

Figure 3. Thermal conductivity.

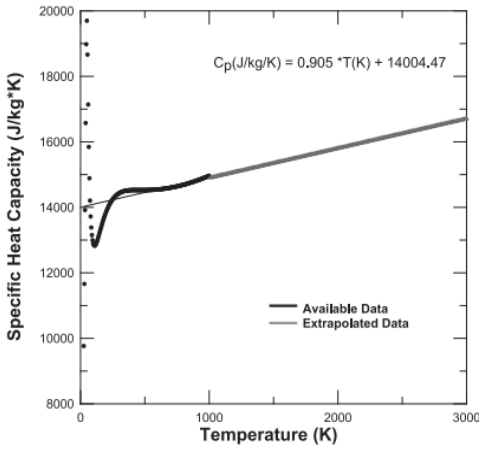

Figure 4. Specific heat capacity.

2.2 Governing Equations

Compressible fluid flow refers to the movement of fluids, such as gases, in which density variations are significant due to changes in pressure, temperature, and velocity. The principles of compressible fluid flow are governed by the fundamental equations of fluid dynamics, which describe the conservation of mass, momentum, and energy principles balance (Siqueira, 2021). For a time-dependent fluid flow, Eq. (1) represents the mass balance, Eqs. (2) to (4) represent the momentum balance in the *x*, *y*, and *z* directions, and Eq. (5) is the energy balance. In these equations, *u*, *v*, *w* refers to the flow velocities in the *x*, *y*, and *z* directions, respectively. And u represents the total vector flow velocity obtained from the sum of the contributions in the x, y, and z directions. The term Φ represents the dissipation function, represented by Eq. (6), and μ is a viscosity term that relates stresses to volumetric deformation. The preceding equations, in their differential form, describe the flow of energy, momentum, and mass at an infinitesimal scale. Given the turbulent nature of the flow, the solver employed in this study adopts a simplified version of these equations, wherein the turbulence model utilized in the calculations presented in this work is based on the Reynolds-Averaged Navier-Stokes (RANS) equations (Ansys, 2021).

$$\nabla.(\rho u) = 0 \tag{1}$$

$$\nabla.(\rho u u) = -\frac{\partial p}{\partial x} + \nabla.(u\nabla u) + S_{Mx} = 0 \tag{2}$$

$$\nabla.(\rho v u) = -\frac{\partial p}{\partial y} + \nabla.(u\nabla y) + S_{My} = 0 \tag{3}$$

$$\nabla.(\rho w u) = -\frac{\partial p}{\partial z} + \nabla.(u\nabla w) + S_{Mz} = 0 \tag{4}$$

$$\nabla.\left(\rho c_p T u\right) = -p\nabla.u + \nabla.(k\nabla T) + \phi + S_i \tag{5}$$

$$\phi = \mu\left\{2\left[\left(\frac{\partial u}{\partial x}\right)^2 + \left(\frac{\partial v}{\partial y}\right)^2 + \left(\frac{\partial w}{\partial z}\right)^2\right] + \left(\frac{\partial u}{\partial y} + \frac{\partial v}{\partial x}\right)^2 + \left(\frac{\partial u}{\partial z} + \frac{\partial w}{\partial x}\right)^2 \left(\frac{\partial v}{\partial z} + \frac{\partial w}{\partial y}\right)^2\right\} + \lambda(\nabla.u)^2 \tag{6}$$

2.3 The description of a Scramjet engine and its cooling channel

In Figure 5, a diagram is presented to indicate the surface location of a Scramjet engine; just below, a two-dimensional conceptual representation of the cross section of that engine is shown. This section is characterized by the attack edge,

followed by the three ramps and channels distributed throughout its structure. The illustration of the cooling channel is present in Figure 6, with its dimensions described as channel width (W), channel height (H), rib thickness (t) and external wall thickness (s) of the heated wall (Bao et al., 2010).

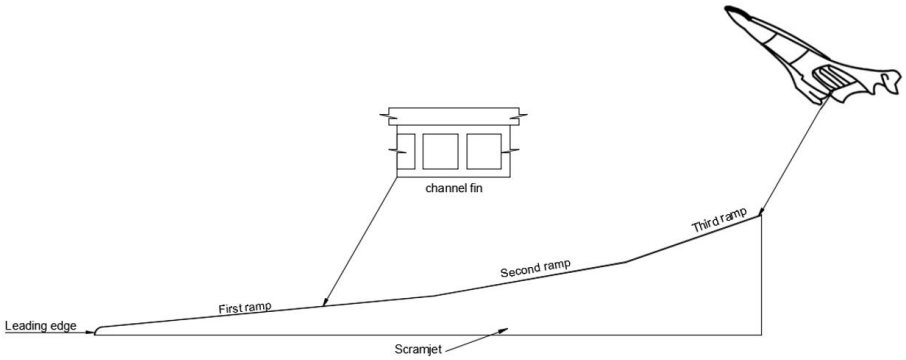

Figure 5. Scramjet engine schematic.

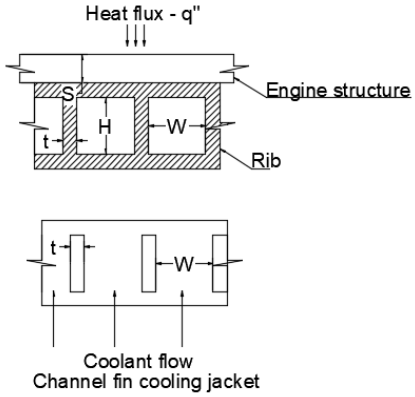

Figure 6. Dimensions that define the characteristics of the cooling channels

2.4 Governing equations of the one-dimensional channel

In the study of the one-dimensional channel, the following fundamental equations are essential to describe the behavior of the system. The parameters characterizing the output temperature can be defined as:

$$q" \, \Delta x \, L \; = \; \dot{m} \, c_p \, (T - T_0) \tag{7}$$

In this equation, $q"$ refers to the thermal flow obtained from the simulation in the fluent. Δx is the width between the centers of the geometric profile, as illustrated in Figure 6. L is the channel length, ṁ is the system mass flow rate divided by the number of channels, C_p is the specific heat and T , T_0 are the input and output temperatures, respectively.

Equation 7(a) provides a more precise simplification.

$$T_{(x)} \; = \; T_0 + \frac{q" \Delta x L}{\dot{m} \, c_p} \tag{7a}$$

The Reynolds number Re is based on the hydraulic diameter, defined as:

$$D_h \; = \frac{4A}{P} \tag{8}$$

Where D_h represents the hydraulic diameter, A denotes the area of the rectangular duct, and P signifies the perimeter.

For the case of friction factor in the laminar regime (Reynolds number, $Re \leq 2300$), this equation is employed.

$$f = \frac{24}{R_{e_{D_h}}} \tag{9}$$

Where f stands for the friction factor, and the Reynolds number Re is calculated based on the hydraulic diameter.

The most utilized expression for calculating the friction factor in turbulent flow conditions $Re \geq 2300$ is the one derived from the Colebrook equation. When determining the roughness of a surface, it is recommended to consider the condition where the ratio of roughness height to hydraulic diameter $\frac{e}{D} \geq 0{,}000001$ (Fox, 2004).

$$\frac{1}{f^{0,5}} = -2{,}0\, log\left(\frac{\frac{e}{D}}{3{,}7} + \frac{2{,}51}{Ref^{0,5}}\right) \tag{10}$$

Equation 11 describes the output pressure of the system and can be defined as follows:

$$P_{(x)} = \frac{f\,\Delta x}{D_h}\frac{v^2}{2} + P_0 \tag{11}$$

Where v represents the velocity, P is the output pressure and P_0 is the input pressure. The other parameters of the equation have already been presented previously.

In this section we derive an important result for the rate of entropy generation in internal flow in a duct of arbitrary geometry with heat transfer at the wall (Bejan, 1996).

The equation 12 yields the entropy generation rate per unit duct length:

$$\dot{S}'_{gen} = \frac{\partial \dot{S}_{gen}}{\partial x} \tag{12}$$

Where $\dot{S}'_{gen} = \frac{\partial \dot{S}_{gen}}{\partial x}$ In applications in which the dimensionless temperature difference τ is negligible as compared to unity we have the simpler form:

$$\dot{S}'_{gen} = \frac{q''L\,\Delta T}{T^2} + \frac{\dot{m}}{\rho T}\left(-\frac{\partial P}{\partial x}\right) \tag{13}$$

When considering the fundamental equations of heat transfer, which are based on the entropy generation rate equations, we proceed to the separate analysis of temperature and pressure gradients, as presented in equations 14 and 15. Through these gradients, it became feasible to obtain values associated with entropy.

$$\dot{S}'_{gen_T} = \frac{q''L\,\Delta T}{T^2} \tag{14}$$

$$\dot{S}'_{gen_P} = \frac{\dot{m}}{\rho T}\left(-\frac{\partial P}{\partial x}\right) \tag{15}$$

3 RESULTS AND DISCUSSIONS

3.1 Channel mesh dependency analysis

Mesh analysis plays a key role in simulating fluid flow in a Scramjet engine operating at high altitudes and supersonic speeds. In this study, we focus our attention on the geometry of the Scramjet engine channel, situated at an altitude of 30 km and operating at a Mach 7 speed. The channel configuration plays a crucial role, affecting both engine performance and flow efficiency. Its main dimensions are a width in the y-axis direction of 2 mm and a total length in the x-axis direction of 800 mm.

The representation of the computational mesh, which describes the channel geometry, is essential for the numerical simulation of the flow. Therefore, it is extremely important that the mesh is properly refined, allowing the precise capture of supersonic flow characteristics and compressibility effects. Figure 7 represents a 2D format where the curvature symbolizes the leading edge and along the x-axis characterizes the surface of the wall, where the darker region corresponds to the refinement near the leading edge and surface of the wall. The mesh shown in Figure x consists of approximately 122,000 cells. And it assists in capturing the boundary layer effects and accurately represents the flow

behavior in these regions through this mesh configuration, the simulation aims to provide reliable and accurate results for the analysis of channel performance and its interaction with flow.

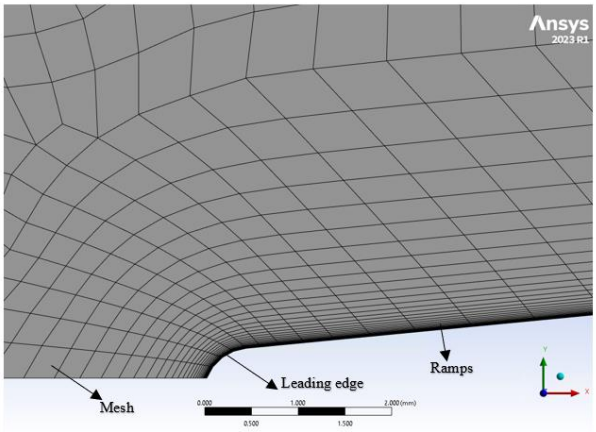

Figure 7. Mesh analysis of the channel

With the definition of the mesh completed, the subsequent step consists in the simulation of the channel geometry. For turbulence calculations, the SSTκ-ω transition model was adopted, taking into consideration an initial wall temperature of 300K. After the initial configuration, the simulation process was performed in the Software ANSYS Fluent, from which the thermal flow values q" was obtained in several coordinates containing information of (x, y and heat flow), for the entire length of the channel wall. These acquired data were subsequently processed using a Python code to calculate the variations of temperature, density, pressure and specific heat. To determine the flow rate and the minimum entropy of the system, it was necessary to use equations 7 to 11.

As previously mentioned, the obtaining of the values of the flow and the minimum entropy of the system was made possible by the implementation of a code in Python. This allowed to calculate these parameters as defined by the established equations. Within this context, Table 1 plays an important role in presenting information related to flow, Reynolds number and entropy, considering temperature and pressure variations. The deduction of entropy values, based on temperature and pressure variations, was performed using equations 14 and 15.

Table 1. Flow rate input data.

Flow	**Reynolds Numbers**	$\dot{S}_{gen}T$	$\dot{S}_{gen}$**P**
ṁ = 0,01	11160,71	0,62284	0,00330
ṁ = 0,015	16741,07	0,44045	0,01066
ṁ = 0,02	22321,43	0,34146	0,02441
ṁ = 0,025	27901,79	0,27904	0,04631
ṁ = 0,03	33482,14	0,23600	0,07813
ṁ = 0,035	39062,5	0,20451	0,12155
ṁ = 0,04	44642,86	0,18045	0,17827
ṁ = 0,045	50223,21	0,16147	0,24996
ṁ = 0,05	55803,57	0,14611	0,33826
ṁ = 0,055	61383,93	0,13342	0,44482
ṁ = 0,06	66964,29	0,12277	0,57129
ṁ = 0,065	72544,64	0,11369	0,71927
ṁ = 0,07	78125	0,10586	0,89041

Using the values presented in columns 2, 3 and 4 of table 1, Figure 8 shows the intersection between the parameters $\dot{S}_{gen}T$ and $\dot{S}_{gen}P$. In this first scenario, the channel geometry with dimensions of 2 mm wide and 2 mm high is being considered.

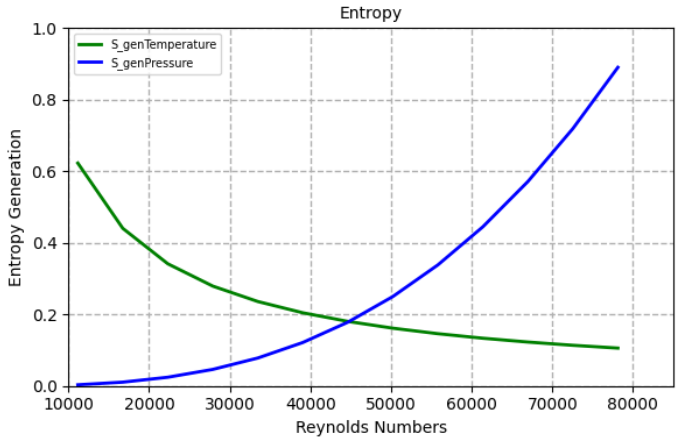

Figure 8. Generation of entropy as a function of Reynolds number.

When analyzing in greater detail the points represented in Figure 8, we can notice that Figure 9 presents a remarkable proximity between the values. This enables an approximate determination of the minimum entropy of the system. This thorough analysis of the data provides a more refined understanding of the results obtained.

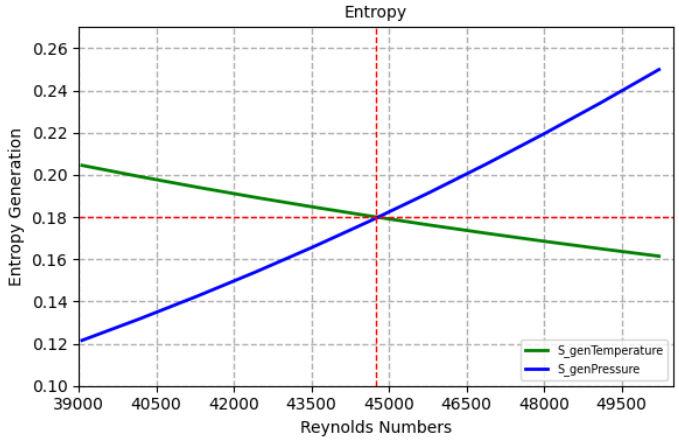

Figure 9. Expansion of the entropy generation.

It is possible to conclude that, in the context of a channel with dimensions of 2x2 mm, the minimum total flow required for the development of the study will be approximately 0.04 kg/s, and the corresponding entropy will be about 0.35872 J/K. This conclusion is supported by Table 1, whose synthesis is presented more concisely in Table 2.

Table 2. Simplification of flow input data.

Flow	**Reynolds Numbers**	$\dot{S}_{gen}$**T**	$\dot{S}_{gen}$**P**
ṁ = 0,04	44642,86	0,18045	0,17827

3.2 Analysis of the channel geometry variation

Initially, the study was conducted considering a scenario in which the channel geometry profile had dimensions of 2x2 mm, resulting in a total flow rate in the system of 0.04 kg/s and an entropy of 0,35872 J/K. Variations in geometry dimensions will now be explored in various scenarios to investigate whether the change in geometric dimensions will affect the flow rate and minimum entropy of the system. Through this analysis, we seek to develop a forecast and thus determine the most appropriate geometric configuration that can lead to a lower entropy and therefore achieve the desired flow.

Figures 10, 11 and 12 will illustrate the variations of the channel geometry profile, considering the dimensions of width and height of 2x3, 2x4 and 2x5, as shown in the images below.

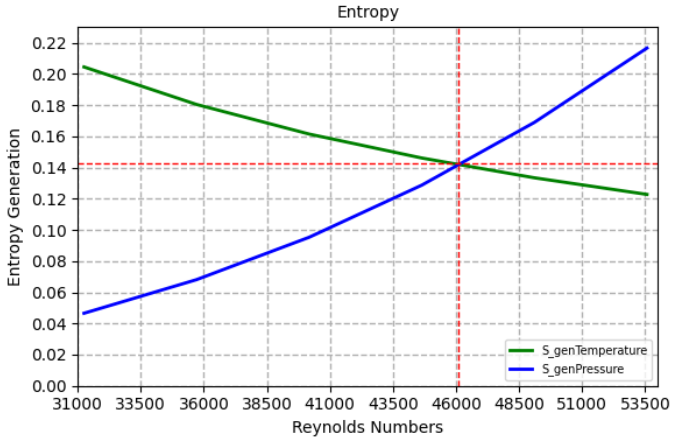

Figure 10. Variation in geometry dimension - 2x3mm

For a channel whose dimensions extend by 2x3 mm, a minimum total flow rate of about 0.05 kg/s is essential. In addition, associated with this condition, the approximate entropy will reach the value 0.27483 J/K.

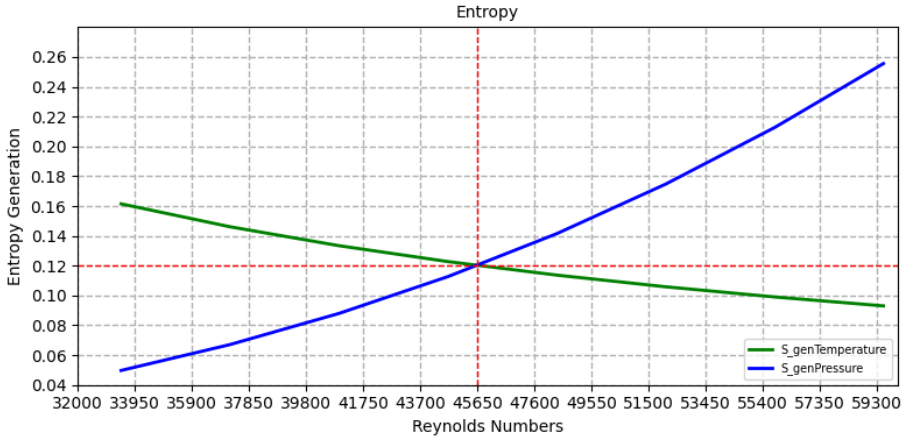

Figure 11. Variation in geometry dimension - 2x4mm

For a channel with 2x4 mm dimensions, a minimum total flow rate of about 0.06 kg/s is essential. In addition, associated with this condition, the approximate entropy will reach the value of 0.23543 J/K.

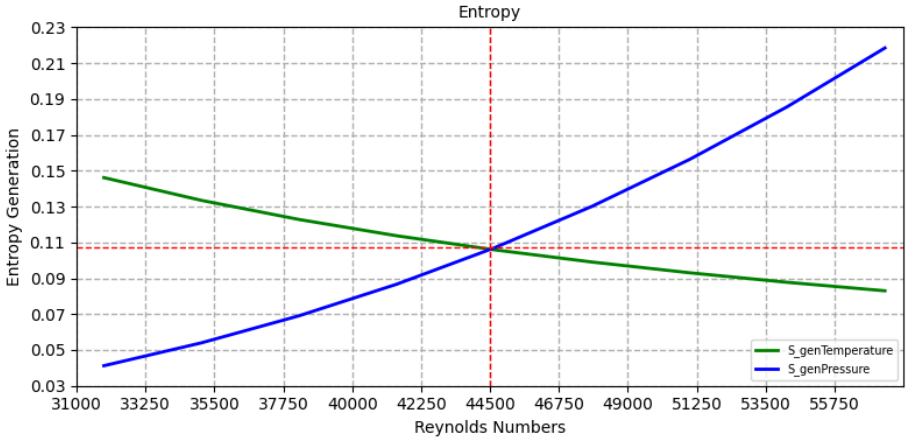

Figure 12. Variation in geometry dimension - 2x5mm

Considering a channel with 2x5 mm extensions, it is essential to ensure that the total flow reaches at least about 0.07 kg/s. In addition, associated with this condition, the approximate entropy will be set at 0.21283 J/K. When examining the different geometric configurations, it becomes evident that the total flow of the system tends to decrease in line with the changes in the channel design. As a result, the Reynolds number, used as an evaluation criterion, also manifests these fluctuations.

From this comparison, it was possible to identify the most appropriate geometric configuration to meet the cooling requirements, aiming at reducing the temperature. This variability in geometry dimensions plays a crucial role in optimizing the cooling system design, ensuring its effective operation and therefore contributing to the safety and efficiency of the engine.

4 CONCLUSION

The implementation of regenerative cooling in Scramjet engines presents a complex approach in solving the high surface temperatures of hypersonic engines. By effectively managing the heat resulting from combustion, this technique aims to improve the performance, reliability and feasibility of more sophisticated aerospace applications.

In order to mitigate these high temperatures, which constitute the initial focus of this article, the main objective was to develop a geometric profile for the channel that was able to initially adapt to the design of the engine. In addition, we sought to determine the optimal minimum flow and entropy required for the successful implementation of this model.

As previously demonstrated, the results were presented throughout this study, and the most appropriate representation of the profile was the geometry of the rectangular channel of 2x2 mm. This option initially revealed greater compatibility with the engine design, resulting in a more accurate match between the flow and entropy associated with this profile.

5 ACKNOWLEDGEMENTS

This work was carried out with the support of the Coordination of Improvement of Higher Education Personnel - Brazil (CAPES) - Funding Code 001, and with support from the National Council for Scientific and Technological Development (CNPq) and with the support of the Program of Academic Cooperation in National Defense (PROCAD-DEFESA), case n. 88881.387753/2019-01.

6 REFERENCES

Ansys, 2021. ANSYS Fluent 21/R2.0 user's guide, Canonsburg.

Bao, W., Qin, J., Zhou, W.X. and Yu, D.R., 2010. Effect of cooling channel geometry on re-cooled cycle performance for hydrogen fueled scramjet. International Journal of Hydrogen Energy, [S.L.], v. 35, n. 13, p. 7002-7011, jul.2010. Elsevier BV. http://dx.doi.org/10.1016/j.ijhydene.2010.04.033.

Bejan, Adrian., 1996. Entropy Generation Minimization. New York: Crc Press, 1996. 389 p

Bonelli, F., Cutrone, L., Votta, R., Viggiano, A., MAGI, V., 2011. Preliminary design of a hypersonic air-breathing vehicle. 17Th Aiaa International Space Planes and Hypersonic Systems and Technologies Conference, [S.L.], v. -, n. -, p. 1-14, 11 abr. 2011. American Institute of Aeronautics and Astronautics. http://dx.doi.org/10.2514/6.2011-2319.

Ferri, A., 1968. Review of scramjet propulsion technology. Journal of Aircraft, [S.L.], v. 5, n. 1, p. 3-10, Jan.1968. American Institute of Aeronautics and Astronautics (AIAA). http://dx.doi.org/10.2514/3.43899.

Fox, R.W., 2004. Introduction to Fluid Mechanics. 6.ed. Danvers: John Wiley & Sons, Inc., 2004. 802 p.

Han, D., Kim, J. S., Kim, K. H., 2022. Conjugate thermal analysis of X-51A-like aircraft with regenerative cooling channels. Aerospace Science and Technology, [S.L.], v. 126, p. 107614, jul.2022. Elsevier BV. http://dx.doi.org/10.1016/j.ast.2022.107614.

He, N., Liu, C., Pan, Y., Liu, J., 2023. Progress of Coupled Heat Transfer Mechanisms of Regenerative Cooling System in a Scramjet. Energies, [S.L.], v. 16, n. 3, p. 1025, 17 jan. 2023. MDPI AG. http://dx.doi.org/10.3390/en16031025.

Labib, S., King, J., 2015. Design and analysis of a single stage to orbit nuclear thermal rocket reactor engine. Nuclear Engineering and Design, [S.L.], v. 287, p. 36-47, jun. 2015. Elsevier BV. http://dx.doi.org/10.1016/j.nucengdes.2015.02.006.

Nasa, 2006. Hyper-X Program Technologies Demonstrates Scramjet X-43A Flight Makes Aviation History A. 2006. Disponível em: https://www.nasa.gov/centers/langley/pdf/142891main_X43A_2006.pdf. Acesso em: 19 jun. 2023.

Siqueira, J.V.M.B., Rosa, M.A.P., Ribeiro, G. B., 2022. Three-dimensional CFD investigation of a scramjet inlet under different freestream conditions. Thermal Science and Engineering Progress, [S.L.], v. 27, p. 101051, jan. 2022. Elsevier BV. http://dx.doi.org/10.1016/j.tsep.2021.101051.

Sun, X., Meng, H., Zheng, Y., 2019. Asymmetric heating and buoyancy effects on heat transfer of hydrocarbon fuel in a horizontal square channel at supercritical pressures. Aerospace Science and Technology, [S.L.], v. 93, p. 105358, out. 2019. Elsevier BV. http://dx.doi.org/10.1016/j.ast.2019.105358.

Walker, M., 2004. Hydrogen and the Scramjet. 2004. Disponível em: https://aerospaceweb.org/question/propulsion/q0170.shtml. Acesso em: 12 abr. 2023.

7 RESPONSIBILITY NOTICE

The authors are the only responsible for the printed material included in this paper.